scientific reports

Check for updates

OPEN

Silencing of PIGU inhibits the progression of esophageal squamous cell carcinoma through the PI3K/AKT signaling pathway

Ji Zuo[1,3], Haiyang Guo[1,3], Guangbing Hu[1,3], Yuman HE[1], Yong Tang[1], Jie Li[1], Yutong Cui[1], Shiqi Liang[1], Xinrui Chen[1], Zichen Luo[1], Xiaobo Wang[1] & Xianfei Wang[1,2]✉

Phosphatidylinositol glycan anchor biosynthesis class U (PIGU), a crucial subunit of the glycosylphosphatidylinositol transamidase (GPI-T) complex, is an oncogene in hepatocellular carcinoma. However, its role in esophageal squamous cell carcinoma (ESCC) remains poorly understood. This study aims to clarify PIGU's role and mechanisms in ESCC by analyzing its expression across pan-cancer datasets, clinical relevance in TCGA-ESCA samples, and effects on cell behavior (migration, invasion, proliferation) and signaling pathways, validated via immunohistochemistry. To examine cell behavior, we used Transwell, colony-formation, CCK-8, and wound-healing assays to assess migration, invasion, proliferation, and wound healing.The epithelial-mesenchymal transition marker levels were measured using Western blot analysis, and the cell cycle and apoptosis were assessed using flow cytometry in conjunction with western blotting. Furthermore, we used western blotting to examine proteins implicated in the PI3K/AKT signaling pathway.To further confirm PIGU's role in ESCC progression, a subcutaneous xenograft mouse model was employed. Our findings suggest that PIGU is highly expressed in ESCC and is strongly associated with tumor growth, lymphatic metastasis and poor prognosis, and is an independent prognostic factor for ESCC patients.PIGU knockdown not only arrested the cell cycle and induced apoptosis, but also significantly reduced migration, invasion, and proliferation in ESCC cells. Additionally, vimentin and N-cadherin were downregulated when PIGU expression was silenced, although E-cadherin expression was simultaneously increased.Moreover, PIGU knockdown decreased the amount of phosphorylated Akt and PI3K. In vivo, PIGU knockdown inhibited ESCC cell proliferation and promoted apoptosis. These findings imply that targeting PIGU may represent a promising therapeutic approach, and that PIGU could potentially serve as both a diagnostic and prognostic biomarker for esophageal squamous cell carcinoma (ESCC).

Keywords PIGU, Esophageal squamous cell carcinoma, PI3K/AKT, Cell cycle, Apoptosis

Esophageal cancer is the 11th most commonly diagnosed cancer and the seventh leading cause of cancer death worldwide, with an estimated 511,000 new cases and 445,000 deaths in 2022[1]. Disturbingly, China bears the greatest burden of this disease, accounting for approximately 50% of all global esophageal cancer cases and deaths each year[2]. Esophageal squamous cell carcinoma (ESCC) is an extremely aggressive and deadly malignancy, predominantly found in Eastern Asia, primarily in China[3]. It poses a significant health burden in the region, warranting immediate attention. The prognosis for advanced ESCC is exceedingly grim, with a 5-year survival rate of less than 20%[4]. ESCC is an especially aggressive malignancy, often diagnosed at an advanced stage, with poor prognosis, resistance to treatment, and a high recurrence rate [5–7]. Current therapeutic approaches, including surgery, chemotherapy, and radiation therapy, have limited efficacy, and the development of resistance to these treatments is a common occurrence[8,9]. Therefore, identifying new therapeutic targets is critical for improving diagnosis, treatment, and outcomes for ESCC patients.

Phosphatidylinositol glycan anchor biosynthesis class U (PIGU), a key subunit of the glycosylphosphatidylinositol transamidase (GPI-T) complex[10], is also known as CDC91L1 or GAB1. The GPI-T

[1]Department of Gastroenterology, Affiliated Hospital of North Sichuan Medical College, Nanchong, Sichuan, China. [2]Digestive Endoscopy Center, Affiliated Hospital of North Sichuan Medical College, Nanchong, Sichuan, China. [3]Ji Zuo, Haiyang Guo and Guangbing Hu contributed equally to this work. ✉email: 2750853458@qq.com

complex facilitates GPI-anchor attachment to proteins, a process critical for cancer progression. The attachment of glycosylphosphatidylinositol (GPI) anchors to their target proteins is facilitated by the GPI-T complex, which is crucial to the development of cancer. The complex is primarily composed of five subunits, with the remaining four being the GPI-anchor attachment 1 proteins, PIG-S, PIG-T, and GPI-8[11,12]. Dysregulation of PIGU has been implicated in several diseases, including cardiovascular disorders[13], dermatological conditions[14], and various cancers[15]. In recent years, PIGU has attracted a lot of interest because of its crucial role in the development and metastasis of cancer[11]. Elevated PIGU expression has been linked to increased motility, epithelial-mesenchymal transition (EMT), and pulmonary metastasis in breast cancer, as well as a poor prognosis[16]. In bladder cancer, higher PIGU levels promote cell proliferation[17], while in thyroid cancer, PIGU overexpression in both tumor cells and tissues facilitates cell proliferation, migration, and invasion[18]. PIGU is similarly overexpressed in hepatocellular carcinoma, where its presence correlates with a poor prognosis. Knockdown of PIGU induces G1-phase cell cycle arrest, suppresses cell proliferation, enhances apoptosis, and inhibits migration and invasion[19]. Despite these findings, the role of PIGU in ESCC remains poorly understood.

The PI3K/Akt signaling pathway, frequently activated in human cancers, plays a crucial role in tumorigenesis and metastatic progression[20–23]. Akt phosphorylation, a key event in this pathway, is facilitated by PI3K, which recruits Akt to the cell membrane[24].Phosphorylated Akt (p-Akt), the active form, is overexpressed in a variety of cancers and is associated with tumor prognosis[25–28]. Once activated, Akt regulates several downstream proteins essential for angiogenesis, migration, cell survival, and proliferation[29,30].

This study identifies significant overexpression of PIGU in ESCC, which correlates with poor prognosis. We also explored the mechanisms by which PIGU contributes to ESCC development. Our findings demonstrate that PIGU is crucial for ESCC cell invasion, migration, and proliferation, suggesting it as a potential therapeutic target for ESCC treatment.

Materials and methods

Collection of datasets

Transcriptomic data and clinical information for 11 normal esophageal tissue samples and 161 esophageal cancer samples were obtained from The Cancer Genome Atlas (TCGA)[31]. The PIGU mRNA expression matrix was extracted for further analysis.

Examining how PIGU mRNA expression and clinical pathological characteristics are related

PIGU expression across various malignancies was analyzed using TIMER2.0[32]. Specifically, in the TCGA-ESCA project, PIGU expression was assessed in esophageal squamous cell carcinomas (ESCCs) and adjacent normal tissues, along with 11 matched esophageal cancer and normal tissue samples. Malignant and normal esophageal tissues' levels of PIGU expression were compared using the GEPIA database[33]. In order to investigate the relationship between PIGU mRNA expression and clinicopathological characteristics in ESCC patients, we also used the R package "ggpubr" to create a clinical correlation heatmap using the TCGA-ESCA dataset.

Prognostic analysis of PIGU mRNA

ESCC patients were stratified into two groups based on their mRNA expression levels, with one group exhibiting high expression and the other exhibiting low expression of PIGU. Kaplan–Meier survival analysis was used to evaluate the prognostic importance of PIGU expression. The predictive accuracy of PIGU expression for one-, three-, and five-year survival outcomes was also assessed using ROC curve analysis. The "Survival" program was employed to conduct univariate and multivariate Cox regression analysis with the objective of identifying independent prognostic markers in ESCC.A nomogram was developed to predict the likelihood of patient survival at 1, 3, and 5 years based on multivariate Cox regression data. The nomogram's accuracy was validated using a calibration plot.

Collection of clinical samples

Clinical information and paraffin-embedded tissue sections from the tumor and surrounding non-tumor tissues were acquired from 80 ESCC patients who had surgery at Chuanbei Medical College's Affiliated Hospital. None of the patients had undergone radiation therapy, chemotherapy, or any other anticancer treatments prior to surgery.Two clinical pathologists verified the esophageal squamous cell carcinoma diagnosis. The North Sichuan Medical College Affiliated Hospital's Medical Ethics Committee approved the study, which was conducted in accordance with the Declaration of Helsinki (permit no: 2024ER562-1).A summary of the clinical characteristics of these 80 patients is provided in Table 1.

Immunohistochemistry

To evaluate PIGU expression in ESCC and nearby non-cancerous tissues, immunohistochemical staining was employed. Tissue sections were dehydrated through graded alcohols after deparaffinization, and then high-pressure steam was used to retrieve the antigen. Goat serum was employed to block non-specific binding, while 3% hydrogen peroxide was used to inhibit endogenous peroxidase activity.For an entire night at 4 °C, sections were treated with a 1:200 dilution of PIGU antibody (Ab192255, Abcam). DAB was used as a chromogenic substrate following the incubation of secondary antibodies. After secondary antibody incubation, DAB was applied as a chromogenic substrate. The sections were then mounted with neutral resin and counterstained with hematoxylin. The immunoreactive score (IRS) was calculated by multiplying the percentage of positively stained cells by the staining intensity. The percentage categories were as follows: < 10% = 1 point, 10%-50% = 2 points, 51%-80% = 3 points, and > 81% = 4 points. Staining intensity was categorized as: poor staining = 1 point, moderate staining = 2 points, and strong staining = 3 points.

Characteristics	Cases	Low expression of PIGU	High expression of PIGU	χ2	P-value
Age				0.031	0.859
< 60	22	13	9		
≥ 60	58	33	25		
Sex				0.108	0.742
Male	43	24	19		
Female	37	22	15		
History of smoking				0.272	0.602
Yes	28	15	13		
No	52	31	21		
History of Alcohol				1.910	0.167
Yes	24	11	13		
No	56	35	21		
Histological grade				1.893	0.388
G1	25	17	8		
G2	52	27	25		
G3	3	2	1		
Location				0.878	0.644
Upper	13	6	7		
Middle	46	27	19		
Lower	21	13	8		
TNM stage				8.451	0.003*
IA + IB + IIA + IIB	41	30	11		
IIIA + IIIB + IVA + IVB	39	16	23		
T stage				10.041	0.001*
T1 + T2	49	35	14		
T3 + T4	31	11	20		
N stage				4.594	0.032*
N0	37	26	11		
N1 + N2 + N3	43	20	23		
M stage				0.047	0.828
M0	78	45	33		
M1	2	1	1		

Table 1. Correlation between PIGU expression and clinicopathological characteristics of ESCC patients. *$p < 0.05$ is significant.

Cell culture and transfection

ESCC cell lines (KYSE510, Eca109, KYSE150, and KYSE30) were obtained from commercial sources. Every cell line was cultivated in media that was enhanced with 1% penicillin–streptomycin solution and 10% fetal bovine serum (FBS). The cells were kept at 37 °C with 5% CO2 in a humidified environment. By cloning the short hairpin RNA (shRNA) sequences into the hU6-MCS-CBh-gcGFP-IRES-puromycin vector, we were able to successfully silence endogenous PIGU expression by infecting the KYSE510 and Eca109 cell lines at a multiplicity of infection (MOI) of 10.Lentiviral vectors were constructed by GeneChem (Shanghai, China). The negative control (NC) sequence, shNC (TTCTCCGAACGTGTCACGT), and the shPIGU sequences—shPIGU#1 (CCT GAGAAACATCTTTGTCCT), shPIGU#2 (GTTTATCCAGATCGCTGTCAT), and shPIGU#3 (GCAATCCAG GACTTCAATAAA)—were employed to knockdown PIGU expression.

RNA extraction and RT-qPCR

Following the manufacturer's instructions, total RNA was extracted from the cells using the RNAex reagent (ACCURATE BIOLOGY) and then reverse transcribed into complementary DNA (cDNA) using the HIScript III RT SuperMix for qPCR (+gDNA wiper) kit (Vazyme). cDNA was amplified by qPCR using the Taq Pro Universal SYBR qPCR Master Mix kit (Vazyme) with the following protocol: initial denaturation at 95 °C for 5 min, followed by 40 cycles of 95 °C for 10 s (denaturation), 60 °C for 30 s (annealing/extension), and melt curve analysis at 65–95 °C[34]. Supplementary material Table 1 contains primer sequences.

Western blotting

Using radioimmunoprecipitation assay buffer enhanced with phosphatase and protease inhibitors, cell proteins were retrieved (Yamei, Shanghai, China). After being resolved using 10% sodium dodecyl sulfate–polyacrylamide gel electrophoresis, the protein samples were transferred to a polyvinylidene difluoride membrane (Millipore, MA, USA) and blocked with 5% non-fat milk for two hours.The primary antibody was incubated overnight at

4 °C, followed by a 1 h incubation with the secondary antibody. Protein bands were detected using the ChemiDoc™ XRS + System (Bio-Rad, CA, USA). Band intensities were quantified using ImageJ software. Information on all antibodies used is detailed in Supplementary material Table 2.

Cell proliferation assay

Utilizing the CCK-8 kit (APExBIO, Houston, USA), cell proliferation was evaluated. A 96-well plate was seeded with 2×10^3 cells per well. A microplate reader was used to quantify absorbance at 450 nm during a two-hour incubation at 37 °C with 5% CO2 following the addition of CCK-8 reagent at 0, 24, 48, and 72 h.

Assays for colony formation were also used to assess cell proliferation. In all, 1,000 cells were cultivated for 12 days at 37 °C with 5% CO2 after being planted in 2 mL of culture media in each well of a 6-well plate. Following fixation with 4% paraformaldehyde for 15 min and crystal violet staining for 10 min, colonies were visualized after multiple phosphate-buffered saline (PBS) washes and air-dried. Colonies were photographed, and colony counts were determined using ImageJ software.

Cell scratch assay

For wound healing assay, 500,000 cells were seeded in each well of a 6-well plate in 2 mL of culture medium and grown to 90% confluence. The cells were cultured in serum-free RPMI 1640 media after the cell monolayer was scratched with a 200-µL pipette tip.To track wound healing, pictures were taken at the same spot at 0 and 24 h.

Migration and invasion assay

Cell migration was assessed using Transwell chambers (8-µm pores, Corning) without Matrigel, while invasion assays were performed using Matrigel-coated Transwell membranes[35,36]. For migration assays, KYSE510 and Eca109 cells were seeded at a density of 50,000 cells per 200 µL in the upper chamber, which contained only basal medium. There were 600 µL of media supplemented with 10% FBS in the lower chamber. Following 48 h of incubation, cells were stained with 0.1% crystal violet and fixed with 4% paraformaldehyde. An inverted microscope was then used to take pictures, and ImageJ software was used to count the number of invasive cells.

For cell invasion assays, Matrigel was applied to the upper chamber prior to cell seeding, and the subsequent procedures were identical to those used for the migration experiments. An inverted microscope was then used to take pictures, and ImageJ software was used to count the number of invasive cells.

Flow cytometry

Cells were digested with a 0.25% trypsin solution and centrifuged at 1000 rpm for 5 min at room temperature. Following two PBS washes of the resultant pellet, 2.0×10^4 cells were preserved with 70% ethanol overnight at 4 °C. The distribution of cell cycles was determined using a cell cycle detection kit (KGA512, KeyGEN BioTECH, Nanjing, China), and flow cytometry (ACEA Biosciences, USA) was employed for analysis.

The Annexin V-APC/Propidium Iodide (PI) Apoptosis Detection Kit (KeyGen Biotech Co., Ltd., Nanjing, China) was used to measure apoptosis in accordance with the manufacturer's instructions. The cells were digested, rinsed twice with PBS, and then resuspended in 500 µL of binding solution in accordance with the cell cycle experiment's instructions. Annexin V-APC and Propidium Iodide (PI), 5 µl each, were added to the cell suspension, and the mixture was incubated in the dark for 10 min. Apoptosis was assessed by flow cytometry (ACEA Biosciences, USA), and apoptosis rates were calculated using FlowJo 10.8.1 software.

Tumor xenograft model

The North Sichuan Medical College Animal Ethics Committee approved the animal study (Approval File Number: 2024092). Male BALB/c mice aged 5 weeks were subcutaneously implanted with 1×10^6 Eca109 cells to generate a xenograft model. Three groups of mice (n = 5) were created: shNC, shPIGU#1, and shPIGU#2. Every five days, measurements of body weight and tumor size were made.For anesthesia, mice were anesthetized using 2–3% isoflurane in oxygen delivered via a vaporizer during all procedures. At the end of the experiment, mice were euthanized by cervical dislocation under deep anesthesia to minimize suffering, in accordance with the committee's guidelines.After 25 days, tumors were excised and fixed in 10% neutral-buffered formalin for subsequent immunohistochemistry (IHC) analysis. The primary antibodies… To compute tumor volume (V), the formula $V = (\text{length} \times \text{width}^2)/2$ was used. Tumor diameter was monitored to ensure it did not exceed 20 mm.

Statistical analysis

For data analysis and graphical display, R software (version 4.3.3) and GraphPad Prism 9.5 (GraphPad Software Inc., San Diego, CA, USA) were utilized. Every experiment was carried out in triplicate, and the mean ± standard deviation is used to express the results. The Student's t-test or one-way analysis of variance (ANOVA) was used to assess differences between two or more groups, and the χ^2 test was used to examine the association between PIGU expression and clinicopathological factors.

To find independent prognostic factors for patients with esophageal squamous cell carcinoma (ESCC), Cox regression analysis was used. Statistical significance was defined as $p < 0.05$($^*p < 0.05$, $^{**}p < 0.01$, $^{***}p < 0.001$, $^{****}p < 0.0001$).

Results

High expression of PIGU in ESCC tissues

We performed a pan-cancer investigation using the Timer2.0 website (http://timer.comp-genomics.org/timer/) and discovered that PIGU was highly expressed in several cancer types, such as colorectal, lung, and esophageal cancers (Fig. 1A). By comparing GEPIA and TCGA-ESCA datasets, we gained deeper insights into PIGU expression in esophageal squamous cell carcinomas (ESCCs) and normal tissues. The results demonstrated a

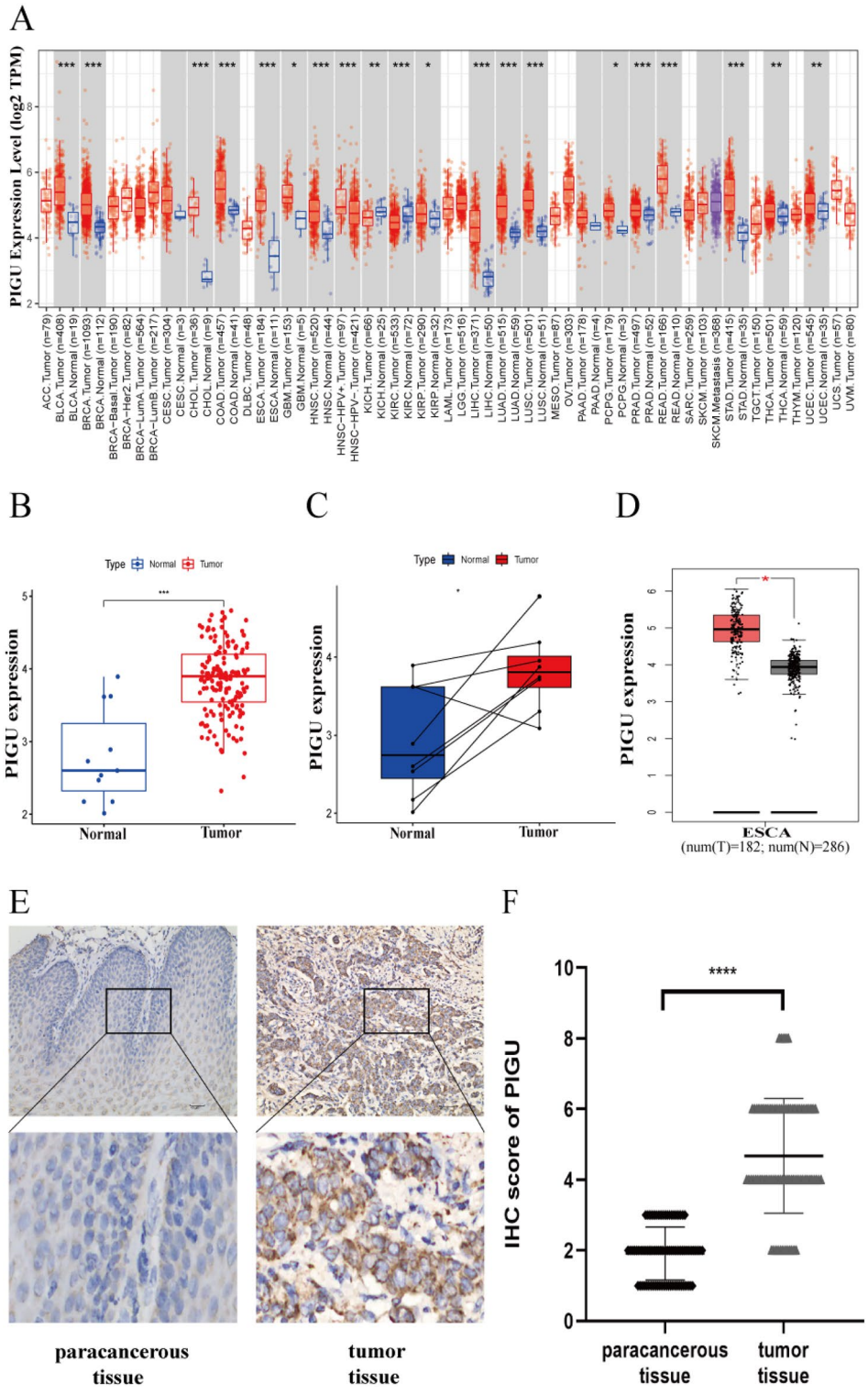

Fig. 1. Expression of PIGU in ESCC and adjacent non-cancerous tissues. **A**–**D** PIGU mRNA expression analyses: **A** Pan-cancer expression via TIMER database; **B**–**C** TCGA-ESCA dataset comparisons between ESCC and normal tissues (B: unpaired; C: paired 11 samples); **D** GEPIA database validation. **E**–**F** PIGU protein expression: **E** Representative IHC images of ESCC and adjacent tissues (×200 magnification); **F** Immunoreactive score (IRS) quantification. $^{*}p < 0.05$, $^{**}p < 0.01$, $^{***}p < 0.001$, $^{****}p < 0.0001$.

notable elevation of PIGU mRNA in cancerous tissues (Figs. 1B, C, and D). Additionally, PIGU is significantly expressed in ESCC tissues, as demonstrated by immunohistochemistry, which revealed that PIGU protein levels were higher in ESCC tissues than in nearby non-cancerous tissues (Figs. 1E and F).

PIGU as a prognostic marker in ESCC patients

Higher levels of PIGU expression in ESCC patients were associated with noticeably worse survival rates, according to Kaplan–Meier survival analysis($p = 0.011$; Fig. 2A). ROC curve analysis revealed AUC values of 0.653 (1-year survival), 0.543 (3-year survival), and 0.790 (5-year survival) for PIGU expression (Fig. 2B). Tumor stage and PIGU expression were identified as significant risk factors for the prognosis of ESCC using univariate and multivariate Cox regression analysis (Figs. 2C and D). A nomogram that incorporated tumor stage and PIGU expression was used to predict overall survival (OS) for patients with ESCC; the 1-, 3-, and 5-year survival rates were 0.965, 0.835, and 0.644, respectively (Fig. 2E). A calibration curve was used to confirm the nomogram's accuracy (Fig. 2F). Based on these findings, PIGU may serve as a significant prognostic factor for patients with ESCC.

Relationship between PIGU and clinicopathological features of ESCC patients

Through the TCGA-ESCA dataset, we further examined the link between PIGU expression and the clinicopathological features of esophageal squamous cell carcinoma (ESCC) patients. Age, gender, and histological grade showed no significant correlation with PIGU mRNA levels (all $p > 0.05$). However, advanced N stage (N0 vs. N1), T stage (T2 vs. T3), and pathological stage (stage I vs. stage III) were significantly correlated with elevated PIGU mRNA expression (all $p < 0.05$; Fig. 3A–F). A clinical association heatmap also revealed significant differences in T stage between the groups with high and low PIGU expression ($p < 0.05$; Fig. 3G). Additionally, we assessed the relationship between PIGU protein levels and clinicopathological features in 80 ESCC patients at our hospital. Using a median immunoreactive score (IRS) of 4, we divided people into groups with low and high expression.Elevated PIGU protein expression was significantly associated with TNM stage ($p = 0.003$), T stage ($p = 0.0015$), and N stage ($p = 0.0321$; Table 1). These findings suggest that PIGU may contribute to ESCC progression by promoting tumor growth and metastasis.

Silencing PIGU inhibits ESCC cell proliferation

In our previous studies, we identified PIGU as a key predictive gene in ESCC. To further investigate its biological role, we examined PIGU expression in four ESCC cell lines (KYSE510, Eca109, KYSE150, and KYSE30). Western blot analysis revealed substantial PIGU expression in KYSE510 and Eca109 cells, which were selected for further studies on PIGU knockdown. (Fig. 4A).Three different PIGU shRNAs (PIGU#1, PIGU#2, and PIGU#3) were transfected into these cells, with PCR and western blot confirming knockdown efficiency, using shNC as a negative control. shPIGU#1 and shPIGU#2 resulted in the most significant reduction in PIGU expression and were selected for further research (Figs. 4B–D). According to CCK-8 assays, the shPIGU#1 and shPIGU#2 groups' proliferative potential of KYSE510 and Eca109 cells was noticeably lower than that of the shNC group (Fig. 4E). Additionally, clonogenic assays demonstrated a marked decrease in colony formation in the shPIGU#1 and shPIGU#2 groups, reinforcing the conclusion that PIGU knockdown inhibits ESCC cell growth (Fig. 4F). These findings emphasize PIGU's potential as a therapeutic target in ESCC by indicating that its silencing inhibits ESCC cell proliferation.

Knockdown of PIGU inhibits EMT in ESCC cells

In addition to demonstrating increased proliferative capacity compared to normal cells, tumor cells undergo epithelial-mesenchymal transition (EMT) more frequently. Our previous research has established a link between PIGU expression and tumor metastasis. To investigate this further, we employed Transwell and cell scratch assays at the cellular level. PIGU knockdown dramatically decreased the migratory and invasive potential of KYSE510 and Eca109 cells, according to both experiments (Fig. 5A, B). EMT, a critical process for tumor invasion and metastasis, is regulated by various factors, as shown in previous studies[37]. To determine if PIGU affects EMT in ESCC cells, we employed western blotting to measure the expression of the mesenchymal markers vimentin and N-cadherin as well as the epithelial marker E-cadherin. The findings demonstrated that in both KYSE510 and Eca109 cells, PIGU knockdown enhanced E-cadherin expression while lowering vimentin and N-cadherin levels (Fig. 5C). These findings suggest that silencing PIGU suppresses EMT in ESCC cells.

Silencing PIGU arrests the cell cycle and promotes apoptosis in ESCC cells

Through cell cycle and apoptosis studies in KYSE510 and Eca109 cells, we further investigated the impact of PIGU on ESCC cell growth. Flow cytometry analysis following PIGU silencing showed a notable increase in the proportion of cells in the G2/M phase (Fig. 6A). We then assessed the expression of key proteins associated with the G2/M phase. PIGU knockdown resulted in decreased levels of Cyclin A2 and CDK1 in both cell lines (Fig. 6B). Next, we examined PIGU's role in apoptosis. The results revealed that silencing PIGU significantly elevated apoptosis rates in both KYSE510 and Eca109 cells (Fig. 6C). Western blot analysis confirmed upregulation of the pro-apoptotic protein Bax and downregulation of the anti-apoptotic protein Bcl-2 after PIGU knockdown (Fig. 6D). According to these results, PIGU silencing hinders the course of the cell cycle and causes ESCC cells to undergo apoptosis.

Silencing PIGU inhibits the PI3K/Akt signaling pathway

The PI3K/Akt pathway, a critical signaling network often dysregulated in cancers, regulates multiple cellular processes including growth, proliferation, differentiation, apoptosis, invasion, metastasis, and EMT[38,39]. Through the PI3K/Akt pathway, silencing Gab1 (PIGU) in hilar cholangiocarcinoma prevents cell migration

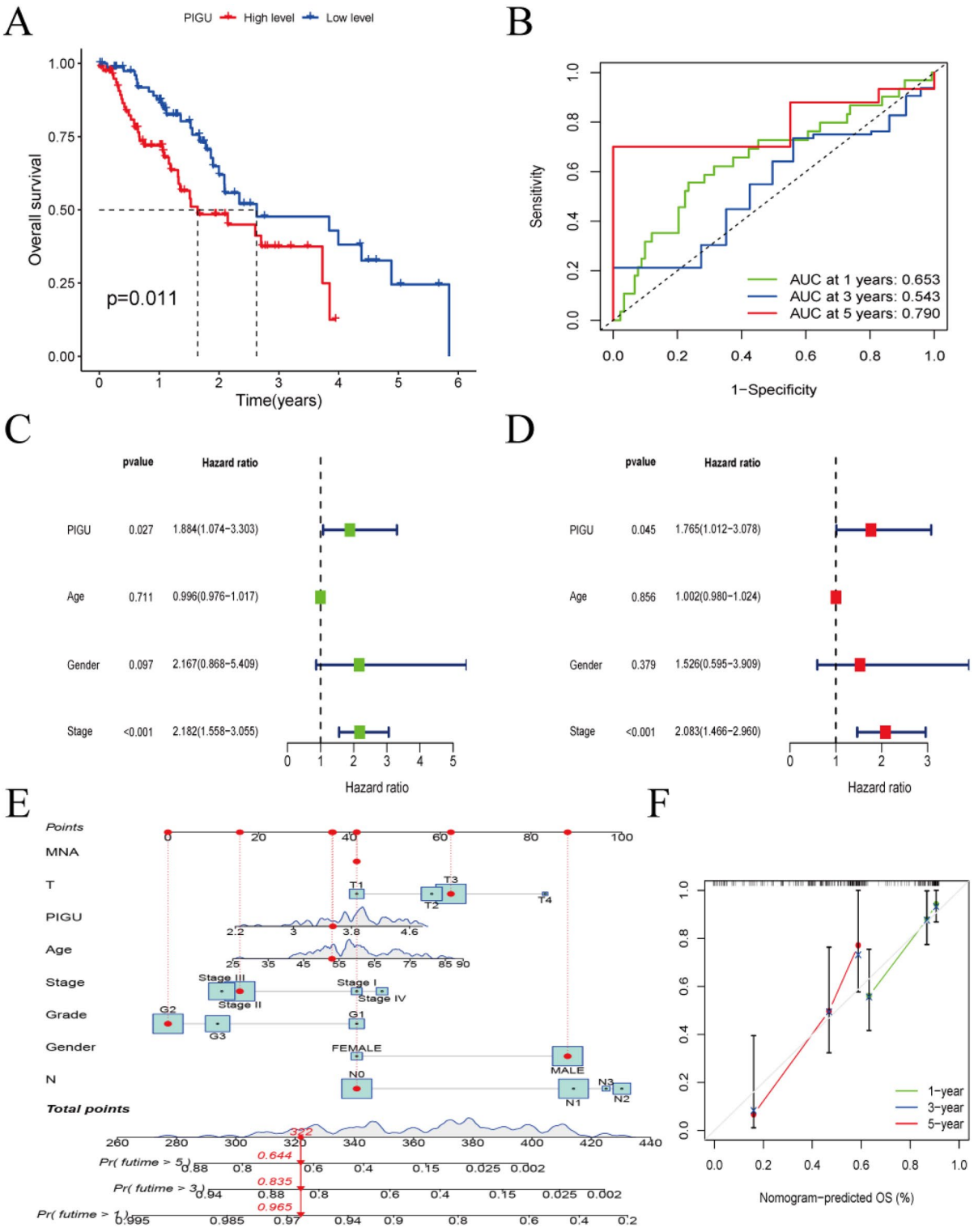

Fig. 2. The prognostic significance of PIGU expression in ESCC patients. **A** Kaplan–Meier survival analysis was used to assess the relationship between PIGU expression and overall survival (OS) in patients with ESCC. **B** ROC curves for PIGU expression predicting 1-, 3-, and 5-year overall survival (OS) in ESCC patients, with AUC values indicated for each time point. **C** and **D** Patients with ESCC are evaluated for prognostic risk factors using univariate and multivariate Cox regression analysis. **E** Nomograms were created to forecast the 1-, 3-, and 5-year overall survival (OS) rates in patients with esophageal squamous cell carcinoma (ESCC) by taking into account PIGU expression levels and disease stage. **F** A nomogram calibration curve is used to verify the nomogram's expected accuracy.*$p < 0.05$, **$p < 0.01$, ***$p < 0.001$, ****$p < 0.0001$.

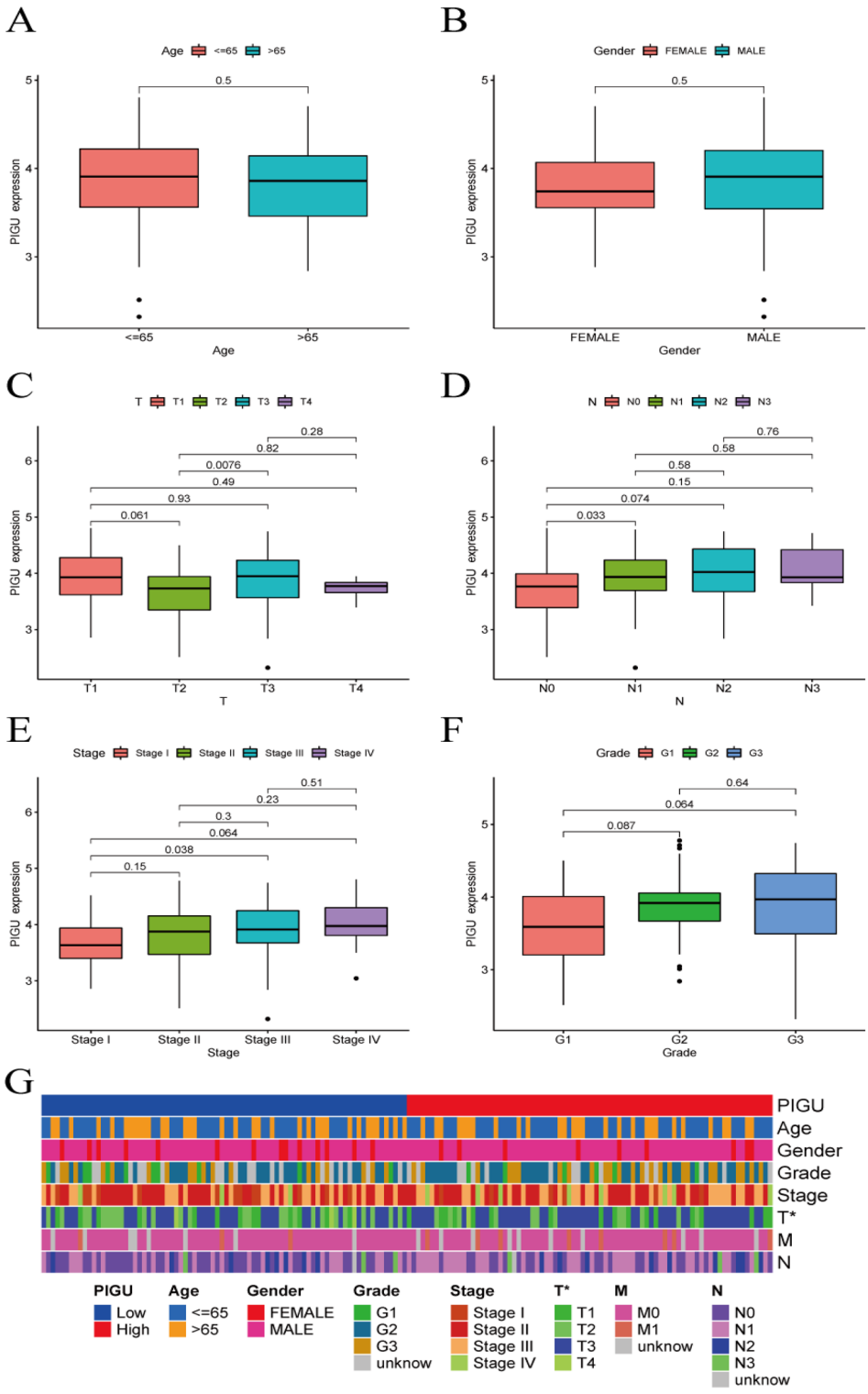

Fig. 3. Relationship between PIGU mRNA Expression and Clinicopathological features using the TCGA-ESCA dataset. **A** Correlation between PIGU mRNA expression and age. **B** Correlation between PIGU mRNA expression and gender. **C** Correlation between PIGU mRNA expression and T stage. **D** Correlation between PIGU mRNA expression and N stage. **E** Correlation between PIGU mRNA expression and pathological stage. **F** Correlation between PIGU mRNA expression and histological grade. **G** Heatmap examination of the clinical connection between clinicopathological characteristics and high/low PIGU expression. $^{*}p < 0.05$, $^{**}p < 0.01$, $^{***}p < 0.001$, $^{****}p < 0.0001$.

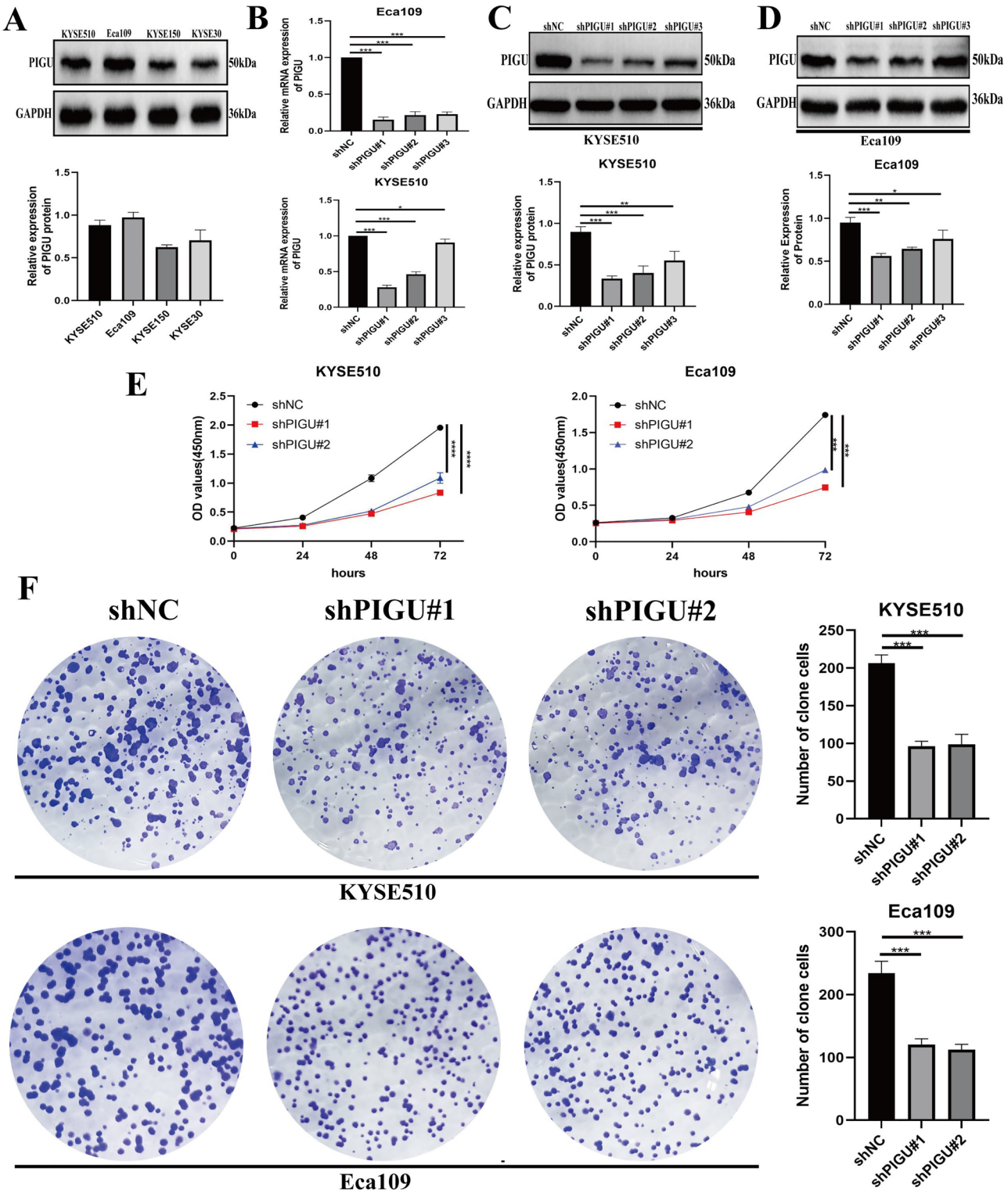

Fig. 4. Relative expression of PIGU in ESCC cells, knockdown efficiency following viral transfection, and effect of PIGU knockdown on ESCC cell proliferation. **A** Expression levels of PIGU protein in different ESCC cell lines. **B** Verification of PIGU knockdown efficiency by RT-PCR. **C** The effectiveness of PIGU knockdown in KYSE510 cells was assessed through Western blot analysis. **D** The effectiveness of PIGU knockdown in Eca109 cells was evaluated by Western blot analysis. **E** CCK-8 assay assessing cell proliferation in KYSE510 and Eca109 cells transfected with shPIGU#1 and shPIGU#2. **F** Clonogenic assay evaluating cell proliferation in KYSE510 and Eca109 cells transfected with shPIGU#1 and shPIGU#2. $^{*}p<0.05$, $^{**}p<0.01$, $^{***}p<0.001$, $^{****}p<0.0001$.

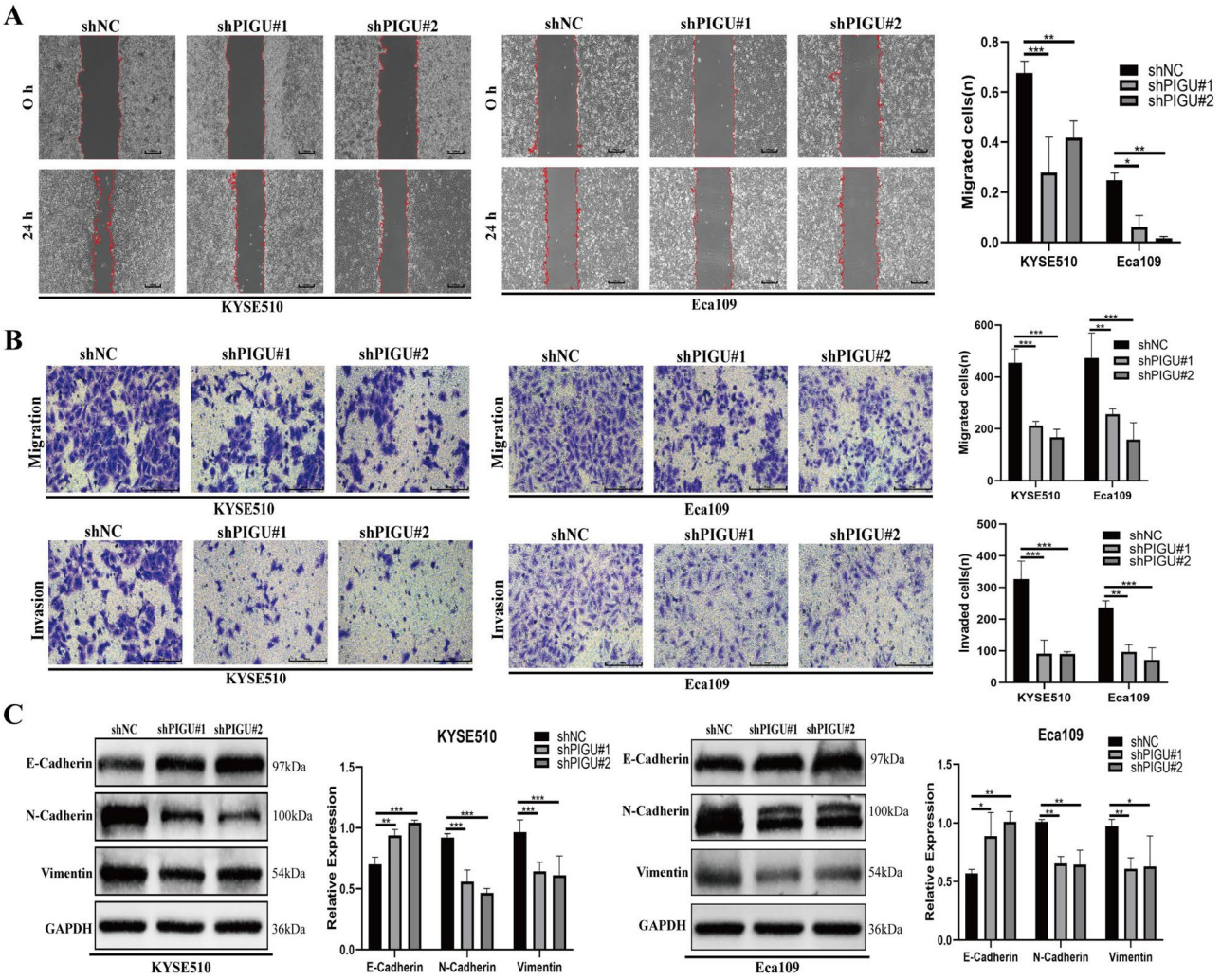

Fig. 5. Knockdown of PIGU inhibits EMT in ESCC cells. **A** The migratory capacity of KYSE510 and Eca109 cells transfected with either shPIGU#1 or shPIGU#2 was evaluated using the cell scratch test.**B** The migration and invasion capabilities of KYSE510 and Eca109 cells transfected with either shPIGU#1 or shPIGU#2 were assessed using Transwell and Transwell (Matrigel) tests.**C** EMT-related markers, such as vimentin, N-cadherin, and E-cadherin, were measured by Western blotting in KYSE510 and Eca109 cells transfected with either shPIGU#1 or shPIGU#2.*$p < 0.05$, **$p < 0.01$, ***$p < 0.001$, ****$p < 0.0001$.

and proliferation[40]. Using PIGU knockdown cell lines, we evaluated the expression of important proteins to see if PIGU influences ESCC cell behavior via this pathway. Our findings demonstrated that silencing PIGU significantly decreased the expression of p-Akt and p-PI3K in both KYSE510 and Eca109 cells as compared to the shNC group (Figs. 7A–C). These findings imply that PIGU may control the development of ESCC by means of the PI3K/Akt signaling pathway.

Silencing PIGU inhibits tumor growth of ESCC in vivo

We conducted xenograft mouse studies to learn more about the function of PIGU in ESCC tumor growth in vivo. After the ESCC tumor model was established, the mice were put to sleep while the tumors were taken out, weighed, photographed, and examined using immunohistochemistry. The results demonstrated that silencing PIGU significantly reduced tumor volume and weight in Eca109 cell-derived tumors (Fig. 8A, B). Immunohistochemical labeling of tumors from shPIGU groups revealed lower levels of PIGU and Ki-67, along with higher expression of Bax and lower expression of Bcl-2, as compared to controls.

Discussion

PIGU, a key component of the GPI-T complex, has been shown to contribute to tumor formation in various cancers[16–19]. Its function in ESCC hasn't been investigated, though. Our study investigates PIGU's biological functions, clinical relevance, and expression pattern in ESCC.

In recent years, The Cancer Genome Atlas (TCGA) has emerged as a core resource for cancer biomarker research, leveraging its pan-cancer multi-omics datasets to drive discoveries. Multiple TCGA-based studies

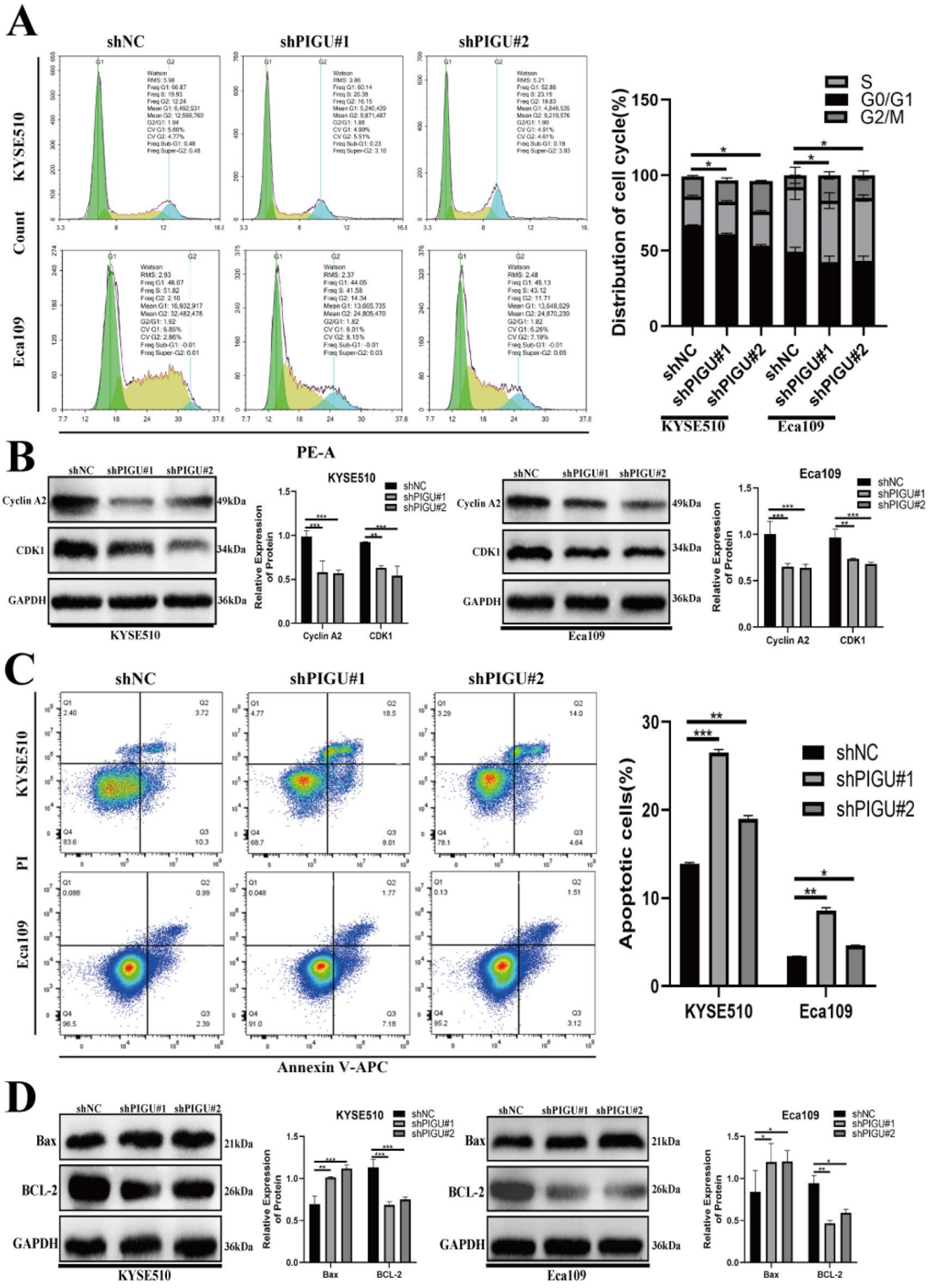

Fig. 6. Silencing of PIGU arrests the cell cycle and promotes apoptosis. **A** The impact of PIGU knockdown on the cell cycle distribution of KYSE510 and Eca109 cells was examined using flow cytometry.**B** The impact of PIGU knockdown on the expression of Cyclin A2 and CDK1 proteins in KYSE510 and Eca109 cells was investigated using Western blotting.**C** Using flow cytometry, the effect of PIGU knockdown on apoptosis in KYSE510 and Eca109 cells is examined. **D** Western blotting analysis of the expression of the proteins Bax and Bcl-2 in Eca109 and KYSE510 cells after PIGU knockdown.*$p < 0.05$, **$p < 0.01$, ***$p < 0.001$, ****$p < 0.0001$.

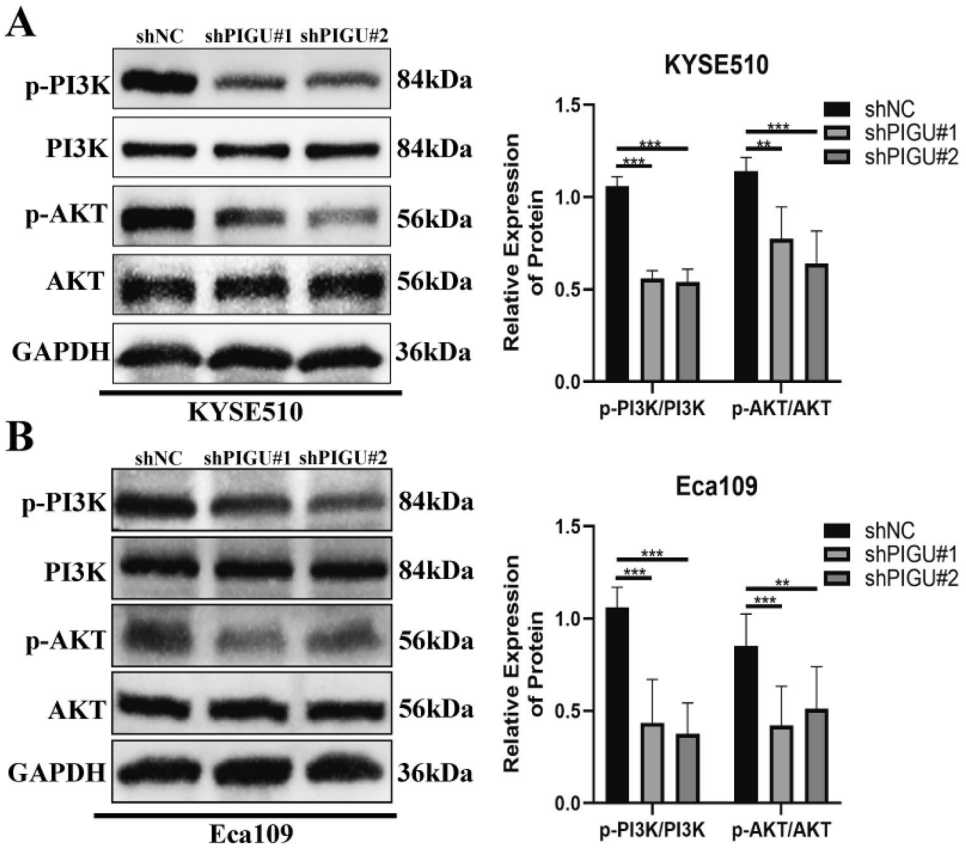

Fig. 7. Silencing PIGU downregulates the expression of PI3K/Akt pathway proteins. **A** The KYSE510 cell line's protein expression in the PI3K/Akt signaling pathway was examined. **B** The expression of proteins in the PI3K/Akt signaling pathway was analyzed in the Eca109 cell line.*$p < 0.05$, **$p < 0.01$, ***$p < 0.001$, ****$p < 0.0001$.

have made significant advancements at both the single-gene and gene-set levels: SCN3B and CDK2 have been identified as potential diagnostic and prognostic biomarkers for glioma[41,42], while AIMP1 and CNIH4 serve as diagnostic and prognostic indicators for head and neck squamous cell carcinoma (HNSC)[43,44]. In specific cancer contexts, IGFBPs exhibit multifunctional value in glioma for diagnosis, prognosis, and treatment prediction[45], whereas the cuproptosis pathway has been linked to kidney renal clear cell carcinoma (KIRC) progression and holds potential for immunotherapy applications[46]. Pan-cancer analyses reveal that CENPA, a key cell cycle biomarker, possesses dual diagnostic and prognostic utility[47]; aberrant expression of VGSC genes suggests their potential as novel pharmacological targets[48]; disulfidptosis-related genes, TRPM7, and RAD51 have respectively emerged as candidate biomarkers for cross-cancer diagnosis/prognosis/therapy, pan-cancer aberrant expression markers, and clinically valuable multi-cancer biomarkers with diagnostic, prognostic, and treatment-predictive capabilities[49–51]. These findings provide new insights into tumor molecular mechanisms. Building on this foundation, our study focuses on the role of PIGU in esophageal squamous cell carcinoma (ESCC), further exploring its scientific significance as a potential biomarker and therapeutic target.

In ESCC tissues, both mRNA and protein levels of PIGU were strongly expressed, corroborating our findings in TCGA and clinical databases. Consistent with the findings of previous studies, elevated PIGU expression has been documented in various cancers, including breast cancer[16], bladder cancer[17], thyroid cancer[18], and liver cancer[19]. The data suggest that high PIGU expression is associated with poorer prognosis, as it increases the likelihood of lymph node metastasis and promotes tumor growth. We hypothesize that PIGU may promote ESCC progression by enhancing the invasiveness of ESCC cells. In support of this, our subsequent in vitro experiments demonstrated that silencing PIGU inhibited both migration and invasion of ESCC cells, while also significantly reducing their proliferative capacity. Previous research has established a strong link between EMT and the migratory and invasive potential of tumor cells[52,53]. Consistent with findings in breast cancer, our study shows that PIGU silencing attenuates EMT in ESCC cells[16]. Tumor progression is critically influenced by the cell cycle[54], with the G2/M checkpoint playing a pivotal role in maintaining chromosomal integrity by ensuring DNA repair before mitosis. CDK1[55] is a crucial regulatory factor at the G2/M phase checkpoint of the cell cycle, while Cyclin A2[56] is a key gene during the G2/M phase. The data confirm that silencing PIGU disrupts the cell cycle by downregulating CDK1 and cyclin A2, leading to a G2/M phase arrest that subsequently impedes ESCC cell proliferation. Furthermore, we found that PIGU silencing significantly enhanced apoptosis in ESCC cells. Flow cytometry analysis revealed a notable increase in apoptotic cells upon PIGU silencing. The protein expression of Bax[57] and Bcl-2[58] proteins—key apoptotic markers—further supported this finding. Specifically, silencing PIGU

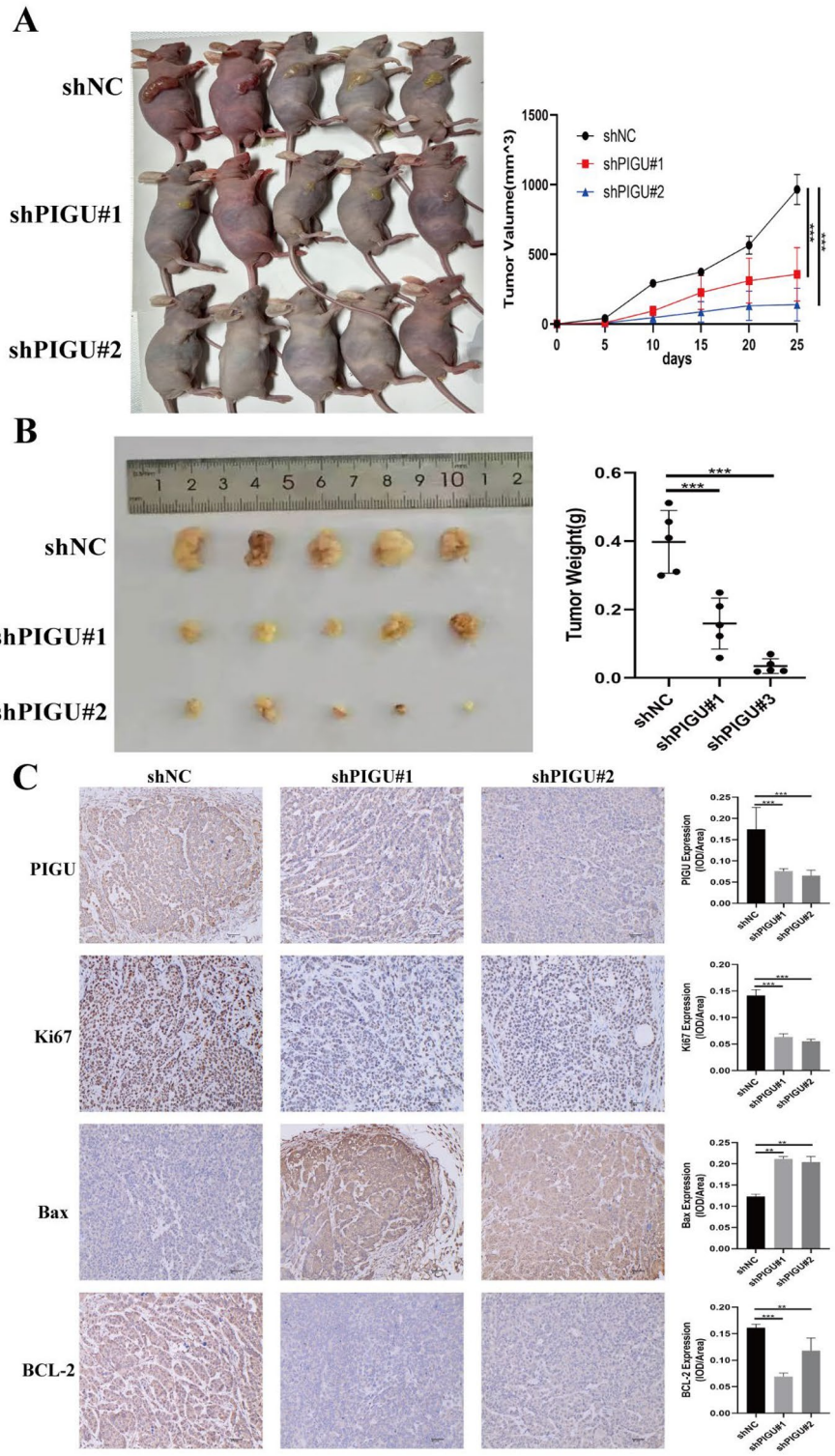

Fig. 8. Silencing PIGU inhibits the growth of ESCC tumors in vivo. (A, B) The volume and weight of Eca109 cell-derived tumors following PIGU knockdown. **C** To assess the expression patterns of PIGU, Ki-67, Bax, and BCL-2 in tumor tissues, immunohistochemical (IHC) examination was done.*$p < 0.05$, **$p < 0.01$, ***$p < 0.001$, ****$p < 0.0001$.

upregulated Bax expression while downregulating Bcl-2, indicating that PIGU silencing promotes apoptosis in ESCC cells.

The PI3K/AKT signaling pathway, a crucial regulator of cell growth, proliferation, invasion, metastasis, apoptosis, and EMT, is often dysregulated in cancers[59,60]. The results show that silencing PIGU reduces the

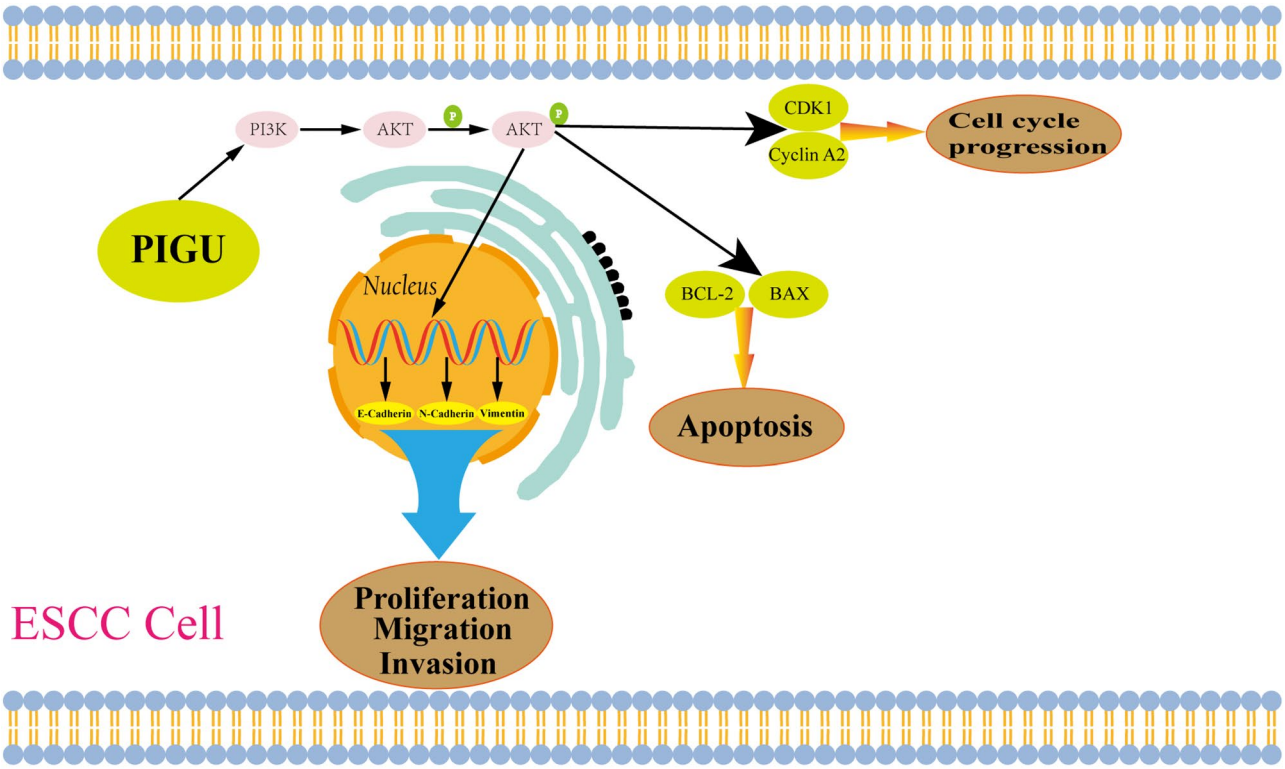

Mechanism diagram. Knockdown of PIGU inhibits proliferation, migration, and invasion of KYSE510 and Eca109 cells through the PI3K/AKT pathway, and blocks the cell cycle and promotes apoptosis.

Fig. 9. Mechanism diagram. Knockdown of PIGU inhibits proliferation, migration, and invasion of KYSE510 and Eca109 cells through the PI3K/AKT pathway, and the cell cycle and promotes apoptosis.

expression of p-AKT and p-PI3K, directly linking PIGU to the activation of this oncogenic pathway in ESCC. These findings suggest that PIGU silencing inhibits ESCC progression through PI3K/AKT pathway suppression. In an in vivo xenograft model, PIGU silencing also suppressed tumor growth. The observed correlation between PIGU and Ki-67 further supports its role in regulating cell proliferation. Additionally, silencing PIGU resulted in upregulation of Bax and downregulation of Bcl-2, reinforcing the promotion of apoptosis Fig. 9. Taken together, our results indicate that PIGU contributes to EMT, proliferation, migration, and invasion in ESCC cells through the PI3K/AKT pathway, while also inhibiting the cell cycle and promoting apoptosis. These findings suggest that PIGU could be a promising therapeutic target for ESCC treatment. However, the potential cross-talk between PIGU and other pathways (e.g., MAPK, Wnt/β-catenin) and its direct interactions with PI3K/AKT components remain to be explored to rule out confounding effects and enhance mechanistic understanding. Moreover, given that PIGU's role may vary across different cancers (e.g., hepatocellular carcinoma[19]), and considering the potential off-target effects of GPI-T complex inhibition, future research should address these issues to ensure the specificity and efficacy of PIGU-targeted therapies.

Beyond its prognostic value, PIGU's strong expression in ESCC tissues implies potential as a diagnostic biomarker, with recent advances in liquid biopsy (e.g., circulating tumor DNA monitoring in neuroblastoma[61]) and molecular barcode technologies (e.g., ultra-sensitive rare tumor cell detection in pancreaticobiliary malignancies[62]), as well as methylation-based non-invasive breast cancer assays[63], offering platforms for non-invasive detection. Speculatively, PIGU mRNA, phosphorylated PI3K/AKT, or exosomal PIGU protein might be detectable in biofluids like plasma via these methods, though validation in independent cohorts is needed to underscore PIGU's translational potential for non-invasive ESCC diagnosis, especially for early-stage detection.

The study has several notable limitations. First, although PIGU overexpression in ESCC was identified using TCGA datasets, bulk RNA-seq data may mask intratumoral heterogeneity and technical biases[64], potentially affecting the generalizability of PIGU's prognostic value across ESCC subtypes. Second, while PIGU knockdown (loss-of-function) was validated in cell lines and xenografts, gain-of-function studies (e.g., PIGU overexpression), particularly in scenarios of gene amplification, are lacking, limiting mechanistic insights. Third, the reliance on established cell lines and xenograft models—without patient-derived organoids or primary tumor explants—hinders recapitulation of ESCC microheterogeneity. Additionally, immune profiling (e.g., tumor-infiltrating lymphocytes) was not performed, precluding understanding of PIGU's interaction with the immune microenvironment. Future studies should incorporate patient-derived xenograft (PDX) models[65] and

single-cell RNA sequencing to address heterogeneity and further investigate PIGU's crosstalk with autophagy, NF-κB, and other signaling pathways (Fig. 9).

Conclusion

In summary, this study establishes PIGU as a pivotal oncogene in esophageal squamous cell carcinoma (ESCC), with its upregulation significantly correlated with tumor progression, lymphatic metastasis, and adverse prognosis. Beyond its utility as a diagnostic and prognostic biomarker, PIGU represents a promising translational target in precision oncology. Key future directions include: 1) developing PIGU-specific inhibitors to disrupt PI3K/AKT-driven tumorigenesis; 2) validating PIGU mRNA or exosomal protein levels in liquid biopsies for non-invasive early detection, leveraging advancements in molecular barcode technologies; and 3) exploring its role as a stratification marker for personalized therapy, particularly in patients with activated PI3K/AKT signaling. Multicenter clinical validation across independent ESCC cohorts and preclinical assessment using patient-derived xenograft (PDX) models are critical to translating these findings into clinical practice. Additionally, combining PIGU-targeted therapies with immunotherapies or chemotherapies may address tumor heterogeneity and improve outcomes for this aggressive disease. Collectively, these insights underscore PIGU's potential to drive the development of innovative diagnostic and therapeutic strategies for ESCC.

Data availability

All raw data are publicly available from corresponding databases. Processed data are available upon reasonable request from the corresponding author.

Received: 26 November 2024; Accepted: 23 June 2025
Published online: 25 August 2025

References

1. Bray, F. et al. Global cancer statistics 2022: GLOBOCAN estimates of incidence and mortality worldwide for 36 cancers in 185 countries. *CA Cancer J. Clin.* **74**, 229–263. https://doi.org/10.3322/caac.21834 (2024).
2. Li, Y. et al. The disease and economic burdens of esophageal cancer in China from 2013 to 2030: Dynamic cohort modeling study. *JMIR Public Health Surveill.* **8**, e33191. https://doi.org/10.2196/33191 (2022).
3. Morgan, E. et al. The global landscape of esophageal squamous cell carcinoma and esophageal adenocarcinoma incidence and mortality in 2020 and projections to 2040: New estimates from GLOBOCAN 2020. *Gastroenterology* **163**, 649-658.e642. https://doi.org/10.1053/j.gastro.2022.05.054 (2022).
4. Zhu, H. et al. Esophageal cancer in China: Practice and research in the new era. *Int. J. Cancer* **152**, 1741–1751. https://doi.org/10.1002/ijc.34301 (2023).
5. Codipilly, D. C. et al. Screening for esophageal squamous cell carcinoma: recent advances. *Gastrointest. Endosc.* **88**, 413–426. https://doi.org/10.1016/j.gie.2018.04.2352 (2018).
6. Sijben, J. et al. Oesophageal cancer awareness and anticipated time to help-seeking: results from a population-based survey. *Br. J. Cancer* **130**, 1795–1802. https://doi.org/10.1038/s41416-024-02663-1 (2024).
7. An, L. et al. The survival of esophageal cancer by subtype in China with comparison to the United States. *Int. J. Cancer* **152**, 151–161. https://doi.org/10.1002/ijc.34232 (2023).
8. Sonkin, D., Thomas, A. & Teicher, B. A. Cancer treatments: Past, present, and future. *Cancer Genet.* **286–287**, 18–24. https://doi.org/10.1016/j.cancergen.2024.06.002 (2024).
9. Liu, H. & Dilger, J. P. Different strategies for cancer treatment: Targeting cancer cells or their neighbors?. *Chin. J. Cancer Res.* **37**, 289–292. https://doi.org/10.21147/j.issn.1000-9604.2025.02.12 (2025).
10. Guo, Z. et al. CDC91L1 (PIG-U) is a newly discovered oncogene in human bladder cancer. *Nat. Med.* **10**, 374–381. https://doi.org/10.1038/nm1010 (2004).
11. Nagpal, J. K. et al. Profiling the expression pattern of GPI transamidase complex subunits in human cancer. *Mod. Pathol.* **21**, 979–991. https://doi.org/10.1038/modpathol.2008.76 (2008).
12. Ohishi, K., Inoue, N. & Kinoshita, T. PIG-S and PIG-T, essential for GPI anchor attachment to proteins, form a complex with GAA1 and GPI8. *Embo. J.* **20**, 4088–4098. https://doi.org/10.1093/emboj/20.15.4088 (2001).
13. Zhang, Z. et al. Gab1 overexpression alleviates doxorubicin-induced cardiac oxidative stress, inflammation, and apoptosis through PI3K/Akt signaling pathway. *J. Cardiovasc. Pharmacol.* **80**, 804–812. https://doi.org/10.1097/fjc.0000000000001333 (2022).
14. Liu, T., Zhang, X. & Wang, Y. miR-183-3p suppresses proliferation and migration of keratinocyte in psoriasis by inhibiting GAB1. *Hereditas* **157**, 28. https://doi.org/10.1186/s41065-020-00138-w (2020).
15. Jiang, W. W. et al. Alterations of GPI transamidase subunits in head and neck squamous carcinoma. *Mol. Cancer* **6**, 74. https://doi.org/10.1186/1476-4598-6-74 (2007).
16. Wang, X. et al. Elevated expression of Gab1 promotes breast cancer metastasis by dissociating the PAR complex. *J. Exp. Clin. Cancer Res.* **38**, 27. https://doi.org/10.1186/s13046-019-1025-2 (2019).
17. Montie, J. E. CDC91L1 (PIG-U) is a newly discovered oncogene in human bladder cancer. *J. Urol.* **174**, 869–870. https://doi.org/10.1097/01.ju.0000171864.79218.0d (2005).
18. Song, P. et al. GAB1 is upregulated to promote anaplastic thyroid cancer cell migration through AKT-MDR1. *Biochem. Biophys. Res. Commun.* **607**, 36–43. https://doi.org/10.1016/j.bbrc.2022.03.101 (2022).
19. Wei, X. et al. PIGU promotes hepatocellular carcinoma progression through activating NF-κB pathway and increasing immune escape. *Life Sci.* **260**, 118476. https://doi.org/10.1016/j.lfs.2020.118476 (2020).
20. Huo, C. et al. eIf3a mediates malignant biological behaviors in colorectal cancer through the PI3K/AKT signaling pathway. *Cancer Biol. Ther.* **25**, 2355703. https://doi.org/10.1080/15384047.2024.2355703 (2024).
21. Gu, J. X. et al. NCAPD2 augments the tumorigenesis and progression of human liver cancer via the PI3K-Akt-mTOR signaling pathway. *Int. J. Mol. Med.* https://doi.org/10.3892/ijmm.2024.5408 (2024).
22. Liu, Y. et al. Let-7 reduces the proliferation and migration of oral cancer cells via PI3K/AKT signaling pathway. *J. Biochem. Mol. Toxicol.* **38**, e23834. https://doi.org/10.1002/jbt.23834 (2024).
23. Ma, Y. et al. KIFC3 promotes the proliferation, migration and invasion of non-small cell lung cancer through the PI3K/AKT signaling pathway. *Sci. Rep.* **14**, 20471. https://doi.org/10.1038/s41598-024-71602-0 (2024).
24. Nussinov, R., Zhang, M., Tsai, C. J. & Jang, H. Phosphorylation and driver mutations in PI3Kα and PTEN autoinhibition. *Mol. Cancer Res.* **19**, 543–548. https://doi.org/10.1158/1541-7786.Mcr-20-0818 (2021).

25. Gan, Y. et al. TDRG1 regulates chemosensitivity of seminoma TCam-2 cells to cisplatin via PI3K/Akt/mTOR signaling pathway and mitochondria-mediated apoptotic pathway. *Cancer Biol. Ther.* **17**, 741–750. https://doi.org/10.1080/15384047.2016.1178425 (2016).
26. Lonetti, A. et al. Improving nelarabine efficacy in T cell acute lymphoblastic leukemia by targeting aberrant PI3K/AKT/mTOR signaling pathway. *J. Hematol. Oncol.* **9**, 114. https://doi.org/10.1186/s13045-016-0344-4 (2016).
27. Sun, B. et al. FDX1 downregulation activates mitophagy and the PI3K/AKT signaling pathway to promote hepatocellular carcinoma progression by inducing ROS production. *Redox. Biol.* **75**, 103302. https://doi.org/10.1016/j.redox.2024.103302 (2024).
28. Liu, T. et al. Splicing factor PTBP1 silencing induces apoptosis of human cervical cancer cells via PI3K/AKT pathway and autophagy. *Front. Biosci. (Landmark Ed)* **29**, 289. https://doi.org/10.31083/j.fbl2908289 (2024).
29. Chu, Y. et al. Co-culture with chorionic villous mesenchymal stem cells promotes endothelial cell proliferation and angiogenesis via ABCA9-AKT pathway. *Faseb. J.* **36**, e22568. https://doi.org/10.1096/fj.202101316RR (2022).
30. Liu, X. et al. Genipin promotes the apoptosis and autophagy of neuroblastoma cells by suppressing the PI3K/AKT/mTOR pathway. *Sci Rep* **14**, 20231. https://doi.org/10.1038/s41598-024-71123-w (2024).
31. Chen, H. et al. Identification of the miRNA-mRNA regulatory network associated with radiosensitivity in esophageal cancer based on integrative analysis of the TCGA and GEO data. *BMC Med. Genomics.* **15**, 249. https://doi.org/10.1186/s12920-022-01392-9 (2022).
32. Li, T. et al. TIMER2.0 for analysis of tumor-infiltrating immune cells. *Nucleic Acids Res.* **48**, W509-w514. https://doi.org/10.1093/nar/gkaa407 (2020).
33. Li, C., Tang, Z., Zhang, W., Ye, Z. & Liu, F. GEPIA2021: integrating multiple deconvolution-based analysis into GEPIA. *Nucleic Acids Res.* **49**, W242-w246. https://doi.org/10.1093/nar/gkab418 (2021).
34. Wu, Z. et al. Icaritin induces MC3T3-E1 subclone14 cell differentiation through estrogen receptor-mediated ERK1/2 and p38 signaling activation. *Biomed. Pharmacother.* **94**, 1–9. https://doi.org/10.1016/j.biopha.2017.07.071 (2017).
35. Liu, H. et al. The voltage-gated sodium channel β3 subunit modulates C6 glioma cell motility independently of channel activity. *Biochim. Biophys. Acta Mol. Basis. Dis.* **1871**, 167844. https://doi.org/10.1016/j.bbadis.2025.167844 (2025).
36. Liu, H., Dilger, J. P. & Lin, J. Effects of local anesthetics on cancer cells. *Pharmacol. Ther.* **212**, 107558. https://doi.org/10.1016/j.pharmthera.2020.107558 (2020).
37. Wei, Q., Qian, Y., Yu, J. & Wong, C. C. Metabolic rewiring in the promotion of cancer metastasis: mechanisms and therapeutic implications. *Oncogene* **39**, 6139–6156. https://doi.org/10.1038/s41388-020-01432-7 (2020).
38. Jiang, N. et al. Role of PI3K/AKT pathway in cancer: the framework of malignant behavior. *Mol. Biol. Rep.* **47**, 4587–4629. https://doi.org/10.1007/s11033-020-05435-1 (2020).
39. Sun, C. et al. F-box protein 11 promotes the growth and metastasis of gastric cancer via PI3K/AKT pathway-mediated EMT. *Biomed. Pharmacother.* **98**, 416–423. https://doi.org/10.1016/j.biopha.2017.12.088 (2018).
40. Sang, H., Li, T., Li, H. & Liu, J. Down-regulation of Gab1 inhibits cell proliferation and migration in hilar cholangiocarcinoma. *PLoS ONE* **8**, e81347. https://doi.org/10.1371/journal.pone.0081347 (2013).
41. Liu, H., Weng, J., Huang, C. L. & Jackson, A. P. Is the voltage-gated sodium channel β3 subunit (SCN3B) a biomarker for glioma?. *Funct Integr Genomics* **24**, 162. https://doi.org/10.1007/s10142-024-01443-7 (2024).
42. Liu, H. & Weng, J. A comprehensive bioinformatic analysis of cyclin-dependent kinase 2 (CDK2) in glioma. *Gene* **822**, 146325. https://doi.org/10.1016/j.gene.2022.146325 (2022).
43. Li, Y. & Liu, H. Clinical powers of aminoacyl tRNA synthetase complex interacting multifunctional protein 1 (AIMP1) for head-neck squamous cell carcinoma. *Cancer Biomark.* **34**, 359–374. https://doi.org/10.3233/cbm-210340 (2022).
44. Liu, H. & Li, Y. Potential roles of cornichon family AMPA receptor auxiliary protein 4 (CNIH4) in head and neck squamous cell carcinoma. *Cancer Biomark.* **35**, 439–450. https://doi.org/10.3233/cbm-220143 (2022).
45. Liu, H. & Tang, T. A bioinformatic study of IGFBPs in glioma regarding their diagnostic, prognostic, and therapeutic prediction value. *Am. J. Transl. Res.* **15**, 2140–2155 (2023).
46. Liu, H. Expression and potential immune involvement of cuproptosis in kidney renal clear cell carcinoma. *Cancer Genet.* **274–275**, 21–25. https://doi.org/10.1016/j.cancergen.2023.03.002 (2023).
47. Liu, H., Karsidag, M., Chhatwal, K., Wang, P. & Tang, T. Single-cell and bulk RNA sequencing analysis reveals CENPA as a potential biomarker and therapeutic target in cancers. *PLoS ONE* **20**, e0314745. https://doi.org/10.1371/journal.pone.0314745 (2025).
48. Liu, H., Weng, J., Huang, C. L. & Jackson, A. P. Voltage-gated sodium channels in cancers. *Biomark. Res.* **12**, 70. https://doi.org/10.1186/s40364-024-00620-x (2024).
49. Liu, H. & Tang, T. Pan-cancer genetic analysis of disulfidptosis-related gene set. *Cancer Genet.* **278–279**, 91–103. https://doi.org/10.1016/j.cancergen.2023.10.001 (2023).
50. Liu, H., Dilger, J. P. & Lin, J. A pan-cancer-bioinformatic-based literature review of TRPM7 in cancers. *Pharmacol. Ther.* **240**, 108302. https://doi.org/10.1016/j.pharmthera.2022.108302 (2022).
51. Liu, H. & Weng, J. A pan-cancer bioinformatic analysis of RAD51 regarding the values for diagnosis, prognosis, and therapeutic prediction. *Front. Oncol.* **12**, 858756. https://doi.org/10.3389/fonc.2022.858756 (2022).
52. Lim, J. & Thiery, J. P. Epithelial-mesenchymal transitions: insights from development. *Development* **139**, 3471–3486. https://doi.org/10.1242/dev.071209 (2012).
53. Brabletz, S., Schuhwerk, H., Brabletz, T. & Stemmler, M. P. Dynamic EMT: a multi-tool for tumor progression. *Embo. J.* **40**, e108647. https://doi.org/10.15252/embj.2021108647 (2021).
54. Atsaves, V. et al. The oncogenic JUNB/CD30 axis contributes to cell cycle deregulation in ALK+ anaplastic large cell lymphoma. *Br. J. Haematol.* **167**, 514–523. https://doi.org/10.1111/bjh.13079 (2014).
55. Wang, Q., Bode, A. M. & Zhang, T. Targeting CDK1 in cancer: mechanisms and implications. *NPJ Precis. Oncol.* **7**, 58. https://doi.org/10.1038/s41698-023-00407-7 (2023).
56. Loukil, A. et al. Cyclin A2: At the crossroads of cell cycle and cell invasion. *World J. Biol. Chem.* **6**, 346–350. https://doi.org/10.4331/wjbc.v6.i4.346 (2015).
57. Liu, Z. et al. Direct Activation of Bax Protein for Cancer Therapy. *Med Res Rev* **36**, 313–341. https://doi.org/10.1002/med.21379 (2016).
58. Campbell, K. J. & Tait, S. W. G. Targeting BCL-2 regulated apoptosis in cancer. *Open Biol.* https://doi.org/10.1098/rsob.180002 (2018).
59. Liu, L., Liu, W. & Deng, W. Amylin inhibits gastric cancer progression by targeting CCN1 and affecting the PI3K/AKT signalling pathway. *Ann Med* **57**, 2480754. https://doi.org/10.1080/07853890.2025.2480754 (2025).
60. Duan, Q., Wang, M., Cui, Z. & Ma, J. Saikosaponin D suppresses esophageal squamous cell carcinoma via the PI3K-AKT signaling pathway. *Naunyn Schmiedebergs Arch Pharmacol.* **398**, 6059–6070. https://doi.org/10.1007/s00210-024-03676-6 (2025).
61. Jahangiri, L. Updates on liquid biopsies in neuroblastoma for treatment response, relapse and recurrence assessment. *Cancer Genet.* **288–289**, 32–39. https://doi.org/10.1016/j.cancergen.2024.09.001 (2024).
62. Ohyama, H. et al. Development of a molecular barcode detection system for pancreaticobiliary malignancies and comparison with next-generation sequencing. *Cancer Genet.* **280–281**, 6–12. https://doi.org/10.1016/j.cancergen.2023.12.002 (2024).
63. Gonzalez, T., Nie, Q., Chaudhary, L. N., Basel, D. & Reddi, H. V. Methylation signatures as biomarkers for non-invasive early detection of breast cancer: A systematic review of the literature. *Cancer Genet.* **282–283**, 1–8. https://doi.org/10.1016/j.cancergen.2023.12.003 (2024).

64. Liu, H., Li, Y., Karsidag, M., Tu, T. & Wang, P. Technical and biological biases in bulk transcriptomic data mining for cancer research. *J. Cancer* **16**, 34–43. https://doi.org/10.7150/jca.100922 (2025).
65. Lee, S. J. et al. hsa-miR-CHA2, a novel microRNA, exhibits anticancer effects by suppressing cyclin E1 in human non-small cell lung cancer cells. *Biochim. Biophys. Acta Mol. Basis. Dis.* **1870**, 167250. https://doi.org/10.1016/j.bbadis.2024.167250 (2024).

Acknowledgements
We are very grateful to the developers of the TCGA public database. We thank the Science and Technology Innovation Center of North Sichuan Medical College and the Institute of Hepatobiliary, Pancreatic and Gastrointestinal Diseases for providing the experimental equipment.

Author contributions
XFW designed the experiments and revised the manuscript. JZ analysed the experimental data and wrote the manuscript. HYG, GBH, YMH and YT performed the experiments. YTC, SQL and JL collected the clinical samples and data. XRC， ZCL and XBW conducted the bioinformatics analysis. All authors have read and approved the final manuscript for publication.

Funding
This research was funded by the Nanchong Science and Technology Program ((grant number: 23JCYJPT0060) and the Key Project of Research and Development Program of Affiliated Hospital of North Sichuan Medical College ((grant number: 2023ZD009).

Declarations

Conflict of interest
The authors declare no competing interests.

Ethics approval
The research adhered to the guidelines outlined in the Declaration of Helsinki, and informed consent was obtained from all human participants included in the study. Approval was received from the Medical Ethics Committee of the Affiliated Hospital of North Sichuan Medical College (Approval File Number: 2024ER562-1).For the animal study, all procedures were reviewed and approved by the North Sichuan Medical College Animal Ethics Committee (Approval File Number: 2024092), and were conducted in accordance with the ARRIVE (Animal Research: Reporting of In Vivo Experiments) guidelines.

Additional information
Supplementary Information The online version contains supplementary material available at https://doi.org/10.1038/s41598-025-08748-y.

Correspondence and requests for materials should be addressed to X.W.

Reprints and permissions information is available at www.nature.com/reprints.

Publisher's note Springer Nature remains neutral with regard to jurisdictional claims in published maps and institutional affiliations.